Evaluation of existing constitutive models in nonlinear 1D effective stress ground response analysis

Caroline Bessette & Samuel Yniesta
Department of Civil, Geological and Mining Engineering – Polytechnique Montréal, Montréal, Québec, Canada

ABSTRACT
The National Building Code of Canada recommends that effective stress ground response analysis be performed if a liquefiable stratum is identified within a soil profile. While constitutive models for total stress ground response analysis have been well verified against earthquake recordings, existing models for effective stress ground response analysis have yet to be thoroughly validated. This paper compares the predictions of five constitutive models derived for effective stress ground response analysis with recordings from downhole arrays and centrifuge tests where a potential for liquefaction was identified during at least one earthquake. The predicted and measured motions are compared in terms of spectral response and ratio of surface to downhole amplification spectra. The results indicate that existing models are limited in their predictive capabilities, and that effective stress ground analysis are not yet a satisfying tool for practicing engineers.

RÉSUMÉ
Le Code National du Bâtiment du Canada recommande une analyse de réponse de sol en contrainte effective lorsqu'un potentiel de liquéfaction est identifié dans un profil de sol. Contrairement à l'analyse de réponse de sol en contraintes totales, les modèles existants n'ont pas été validés à ce jour avec des enregistrements de séismes. Cette étude compare les prédictions de cinq modèles constitutifs dérivés pour l'analyse de réponse de sol en contraintes effectives avec des enregistrements provenant de stations d'accéléromètres et de tests en centrifuge, où un potentiel de liquéfaction a été identifié pour au moins un séisme. Les réponses mesurées et prédites sont comparées par l'entremise de la réponse spectrale et du spectre d'amplification entre la surface et la profondeur. Les résultats indiquent que les modèles sont limités dans leur précision et qu'une analyse de réponse de sol en contrainte effective ne constitue pas encore un outil satisfaisant pour assister les ingénieurs dans la pratique.

1 INTRODUCTION

Ground response analyses are performed to evaluate how local site conditions will affect the propagation of an earthquake motion. Upon undrained cyclic loading conditions, induced excess pore water pressures develop which result in significant degradation of the material's stiffness and strength and alteration of the stress wave propagation. For saturated loose cohesionless soils, the generation of pore pressure is problematic as it can lead to liquefaction. Consequently, when a liquefaction potential is identified within a soil profile, the National Building Code of Canada recommends a site-specific effective stress ground response analysis. However, the current state of practice in ground response analysis revolves around well-established total stress simulations which have seen extensive validation efforts. For example, a prior benchmarking study by Kaklamanos et al. (2015) used 191 ground motions with varying ground motion amplitudes from six Kik-net sites to evaluate the site response models' uncertainties. The major issue is that total stress analysis does not consider pore pressure generation, while only few effective stress models have been developed. The use of effective stress models remains limited due to the fact that few studies have been reported that validate these models against recordings of earthquake events of both low and large amplitudes.

The objective of this study is thus to provide a comprehensive investigation of the predictive capabilities of effective stress models in 1D ground response analysis using the program Deepsoil developed by Hashash et *al.* (2016). This is accomplished by comparing the predictions from five effective stress constitutive models against seven liquefaction case studies, including downhole array recordings and centrifuge experiments. A total of 55 earthquake recordings with a broad range of nonlinearities and levels of pore pressure generation were simulated.

This project provides an opportunity to better understand the effect of liquefaction on ground motion propagation, and address the gap between the theoretical soil models developed and their potential use in practice. The long-term objective of this study is to develop guidelines for accurately performing effective stress ground response analysis in practice.

This paper first reviews the effective stress approach in 1D ground response analysis and offers a literature review of the existing models for predicting the pore pressure buildup during cyclic loading. This will be followed by a description of the case studies and the modelling approach. An example of the comparison between the site response codes will be presented with a case study analysis of the 1987 Superstition Hills Earthquake recorded at the Wildlife Liquefaction Array site. The bias and variability of the predictions are then quantified statistically using mixed-effect regression analysis and Pearson's correlation coefficients in order to compare the observed and predicted surface spectral acceleration and the ratio of surface to downhole amplification spectra.

2 EFFECTIVE STRESS ANALYSIS

Effective stress soil constitutive models, which couple modulus reduction and damping curves with degradation index functions, developed by Matasovic (1993) for sands and Matasovic and Vucetic (1995) for clays, must be used in conjunction with models that allow the modeling of generation, redistribution and dissipation of excess pore pressure. This section reviews some of the existing models for both granular and cohesive soils and their limitations.

2.1 Granular soils

Stress-based models

The first models for the study of pore pressure generation were based on cyclic stress-controlled laboratory testing. Lee and Albaisa (1974), Seed et *al*. (1975) and Booker *et al*. (1976) developed simple empirical models which expressed the excess pore pressure ratio (r_u) with the cyclic ratio (N/N_L), where N is the number of loading cycles and N_L is the number of cycles required for the initiation of liquefaction. Park and Anh (2013) proposed a simplified model based on the concept of a damage parameter to account for the accumulation of stress and can be used in absence of strain-controlled testing as it requires only the cyclic stress ratio vs the number of cycle (*CSR*-*N*) curve obtained by stress-controlled testing, as given in Equation 1.

$$r_u = \frac{2}{\pi} arcsin\left(\frac{D}{D_{ru=1.0}}\right)^{\frac{1}{2\beta}} \quad [1]$$

where D is the damage parameter, CSR_t is the threshold shear stress ratio, β is a fitting parameter and $D_{ru=1.0} = 4N(CSR - CSR_t)^{\alpha}$.

Strain-based models

Laboratory testing by Youd (1972), Silver and Seed (1971) and Pyke (1975) later found that the controlling factor of pore water pressure generation is cyclic strains rather that cyclic stresses. They also discovered the existence of a volumetric threshold shear strain γ_{tvp} below which no pore pressure is generated. Dobry et *al*. (1985) proposed a model which was later modified by Vucetic and Dobry (1986):

$$u^*_N = \frac{p \cdot f \cdot F \cdot N(\gamma_c - \gamma_{tvp})^s}{1 + f \cdot F \cdot N(\gamma_c - \gamma_{tvp})} \quad [2]$$

where *p, F, s* are curve fitting parameters, *f* accounts for the number of dimensions, *N* is the number of cycles and γ_c/γ_{tvp} are respectively the current and threshold cyclic shear strains. Carlton (2014) and Mei et *al*. (2018) developed correlations for the estimation of *s* and *F* parameters based on shear wave velocity, fines content and relative density.

Energy-based models

Energy-based models relates the dissipated shear energy per unit volume of soil to the residual excess pore pressure ratio (r_u). The table below presents two of the available energy-based models.

Table 1. Energy-based Effective stress models

Model	Equation	
GMP – Green et *al*. (2000)	$r_u = \alpha\sqrt{\frac{W_s}{PEC}}$	[3]
Generalized – Berrill and Davis (1985)	$r_u = \alpha \cdot {W_s}^{\beta}$	[4]

where the dissipated energy (W_s) is defined as the area bounded by the stress-strain hysteresis loops and α and β are fitting parameters. *PEC* is a calibration parameter evaluated as a function of the relative density and fines content derived by Polito et *al*. (2008).

2.2 Cohesive soils

For clays, degradation is not only a result of excess pore pressure but also of microstructure deterioration due to the breakage of particle bonds, as found by Matasovic and Vucetic (1995) which proposed a 1D strain-controlled model expressed as

$$u_N{}^* = AN^{-3t} + BN^{-2t} + CN^{-t} + D \quad [5]$$

where *N* is the number of loading cycles, *A, B, C* and *D* are fitting parameters, $t = s(\gamma_c - \gamma_{tvp})^{v}$ and v is a degradation parameter as defined by Matasovic (1993).

2.3 Limitations

Most of the discussed models are empirical or semi-empirical and are based on experimental results. However, limited work is available on the validation of their predictions. The main issue is the large number of input parameters and the little guidance in literature to select these parameters in the absence of laboratory test data. Thus, as most of the tests are performed on clean saturated sands, it is difficult to assess if a model is able to produce reliable estimations of excess pore pressure buildup in soils with a wide range of properties such as fines content and granulometry. In addition, limitations in the modelling assumptions do not allow for the consideration of the dilative response observed during liquefaction. The dilative tendency results in a strain-hardening response and an increase in the soil's stiffness which enables the propagation of a significant portion of the ground motion sometimes associated with high amplitude high frequency acceleration pulses (Brandenberg et *al*., 2013). Other in-situ factors are also neglected, such as multidirectional shaking, upward seepage, presence of static shear stresses, etc.

3 DATA

The predictive capabilities of the effective stress models are studied by simulating the ground motion propagation at five sites with downhole arrays and in two centrifuge tests. In all seven case studies, several ground motions of various amplitudes were recorded with a least one motion generating significant pore pressure and triggering liquefaction, except for one case. In total, 55 ground motions were selected for the seven case studies with 13 motions triggering liquefaction. The following section presents a brief description of the selected case studies.

All case studies are instrumented with a minimum of a pair of seismometers located at some depth in a borehole and at the ground surface. Thus, in ground response analysis the downhole record can be used directly as an input motion and the resulting surface motion can be compared with the observed recordings for validation purposes. A few case studies also have pore pressure transducers to record the generation of excess pore water pressure. For the sites with no installation of pore pressure transducers, time-frequency analysis of the observed ground surface motion is performed to identify liquefaction using the Stockwell transform (Stockwell et *al.* ,1996). Previous research by Kramer et *al.* (2018) suggests that an abrupt change in the frequency content over time may be associated with a triggering of liquefaction.

First, two sites were selected from the Kiban-Kyoshin (KiK-net) strong-motion network of vertical high sensitivity seismographs arrays (Hi-net) located in Japan. Site KSRH07 has a total depth of 224 m and consists of interbedded layers of sand, sandy gravel, pumice and volcanic sand over sandstone and conglomerate. The average shear wave velocity in the upper 30 meters ($V_{s\text{-}30}$) is 300 m/s. Time-frequency analysis did not reveal any evidence of significant pore pressure generation, but a simplified liquefaction analysis (Kayen et *al*., 2013) yields a probability of liquefaction of almost one for two motions.

The second Kik-net Site (TCGH16) is 112 m thick and consists of interbedded layers of sand, clay, gravel and sandy gravel over sandstone and mudstone and the $V_{s\text{-}30}$ *is 285* m/s. Time-frequency analysis revealed possible liquefaction for one of the events with an abrupt change in the frequency content in the surface motion compared with the downhole motion. The simplified liquefaction analysis revealed a probability of liquefaction of almost one for three of the motions. For each sites, the eight recorded motions with the highest amplitudes were selected, having *PGA* values at the surface ranging from 0.07 to 1.0 *g* and magnitude M_w>4.9.

The third site is the Wildlife Liquefaction Array (WLA) situated in the Imperial Valley in Southern California. This site is a well-documented case study of observed liquefaction where multiple geotechnical investigations were conducted (e.g. Bennett et *al*., 1984; Youd and Holzer 1994; Youd et *al*. 2004). The USGS first instrumented the site in 1982 with surface and downhole accelerometers and six piezometers. In November 1987, the piezometers recorded a pore pressure ratio of 100% for the Superstition Hills earthquake. In 2004, the site was re-instrumented as part of the NEES program with 9 accelerometers and 8 piezometers. The site consists of a 4.3 m thick liquefiable layer of silty sand bounded by a silt and a clay to silt layer on top and bottom. The shear wave velocity of the profile varies from 100 (0-2.5m) to 116 m/s (2.5-7.5m). The downhole accelerometer is located at a depth of 7.5 m. A total of twelve recordings were selected from this site.

The fourth site is the Lotung site or LSST in Taiwan. The soil profile consists of 47 m of interbedded silty sand, clayey silt, gravel and organic matter. Velocity profile are obtained from EPRI (1993) and the $V_{s\text{-}30}$ *is* 193 m/s. Accelerometers are installed at the surface and at 6, 11, 17 and 47 m. From the 10 selected events, 4 earthquakes are associated with a high probability of liquefaction evaluated with a simplified liquefaction analysis.

The final downhole array site is located at Port Island, a reclaimed island in Kobe Port, Japan. In 1991, the Development Bureau of Kobe City instrumented the site with four accelerometers located at the ground surface and at depths of 16, 32 and 83 m. On January 17, 1995, the mainshock Hyogo-ken Nanbu (Kobe) Earthquake was recorded and caused liquefaction of the saturated surficial fill which consists of decomposed granite, gravel and sand. This layer is underlaid at 19 m by interbedded layers of alluvial clay, sand, sand with gravel and diluvial clay. Suspension P-S velocity logging was performed to obtain velocity profiles where $V_{s\text{-}30}$ *is* 198 m/s, in addition to a standard penetration test for N values (Iwasaki and Tai, 1996). Besides the main Kobe motion, a foreshock and an aftershock were used in the analysis.

Finally, two centrifuge tests where liquefaction was triggered were selected. Because of their geometries, the two tests were deemed to be representative of a 1D ground motion propagation problem. For both tests, pore pressure transducers and accelerometers are installed at various depths. First, free-field centrifuge test data from Wilson et *al*. (2000) is used (referred as test CSP3), where the soil prototype consists of two layers of saturated fine, uniformly graded Nevada Sand. The top and bottom layers have a relative density D_r of 55% and 80% and a thickness of 9.3 m and 11.4 m respectively. The tests were conducted at a centrifugal acceleration of 30*g*. The shear wave velocity profile was defined based on Bardet et *al.* (1993), with a minimum value of 120 m/s. A total of ten earthquake motions were used based on scaled recordings of the Kobe earthquake at Port Island station and the Loma Prieta earthquake at the University of California at Santa Cruz.

The final case study, CFF2 uses centrifuge free-field conditions results from Olarte et *al*. (2017) and Kirkwood and Dashti (2018). The model is composed of a 2 m thick layer of Monterey sand 0/30 with a relative density of 90%. This top layer is underlaid by two layers of Ottawa sand F65 of 6 m and 10 m thick at a relative density of 40% and 90% respectively. A nominal centrifugal acceleration of 70*g* was applied. Six scaled motions were used from the Joshua Earthquake recorded at the station Joshua Tree, Kobe at Takatori station and Northridge at Newhall-WPC station.

4 METHODOLOGY

This section describes how the ground response analysis presented in this investigation were performed, how the models were calibrated, and how the results were analyzed in order to assess the accuracy of each model.

4.1 Ground response models

In this study, total stress equivalent-linear (EQL), total stress nonlinear (NL-TS) and effective stress nonlinear (NL-ES) analyses were conducted using the software Deepsoil v6.1.1 developed by Hashash et *al*. (2016). First, the shear wave velocity profiles of each site were verified with total stress nonlinear analysis by simulating a small amplitude motion and comparing the surface response spectrum obtained with the recorded one. The target modulus reduction and damping curves of Zhang et *al*. (2005) were used for all sites. The General Quadratic/Hyperbolic model (GQ/H) with strength control (Groholski et *al*. 2016) was employed with MRDF-UIUC unload-reload rules (Phillips and Hashash 2009). The shear strength of granular and cohesive soils was defined by the Mohr-Coulomb criterion and Ladd (1991) relationship respectively. The small-strain damping formulation was taken as frequency independent (Phillips and Hashash 2009). A rigid boundary condition was considered for all sites because within motions are used. For recordings with both horizontal orthogonal components available, the geometric mean was used to combine the results. All ground motion records were high-pass and low-pass filtered, and baseline corrected.

Table 2. Pore pressure generation models (see Section 2.1)

ID	Model	Equation
M1	Dobry & Matasovic	2
M2	GMP	3
M3	Park & Anh	1
M4	Generalized	4

For the effective stress models, the four models presented in Table 2 are used. The calibrations were made based on available site properties, recommendations by the authors of the published models or general correlation relationships mentioned in Section 2.1. Finally, soil layers which consist of cohesive soils were represented by the Matasovic and Vucetic (1995) model.

4.2 Model validation methods

In order to quantify the accuracy of the predictions of a given ground response simulation, the observed surface response spectra was compared to the predicted spectra by computing the residual defined by Equation 6.

$$PSA_{res}(T) = ln[PSA_{obs}(T)] - ln[PSA_{pred}(T)] \quad [6]$$

where *PSA* is the 5%-damped pseudo-acceleration spectra. Note that a positive residual indicates an under-prediction

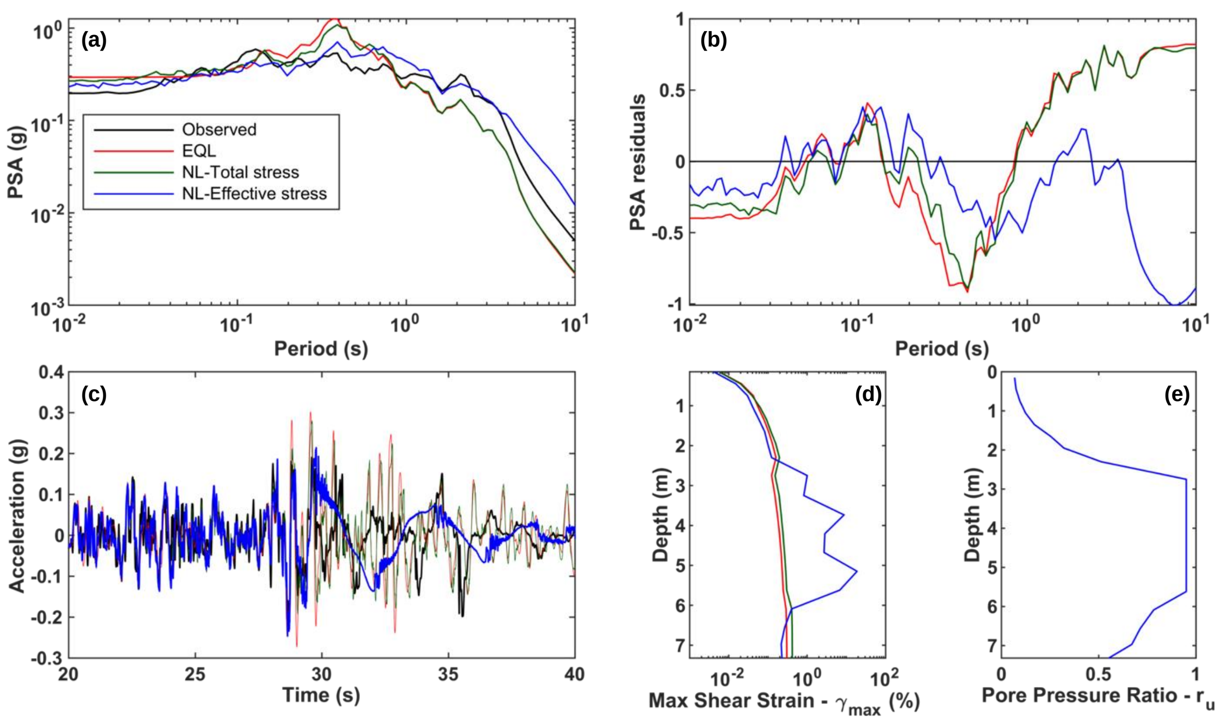

Figure 1. Detailed liquefaction case study example for the Superstition Hills Earthquake at the WLA site. Results from total stress equivalent-linear (EQL), total stress nonlinear (NL-TS) and effective stress nonlinear (NL-ES) analysis with GMP model (M2): (a) Pseudo-acceleration surface response spectra, (b) Response spectra residuals, (c) Surface acceleration time histories, (d) Maximum shear strain profile and (e) Pore pressure ratio profile with depth for the NL-ES analysis.

and a negative residual refers to an over-prediction of the motion.

The residuals were computed across multiple sites and ground motions, and a statistical analysis was performed to evaluate the uncertainties of the site response models. Linear mixed-effect regression analysis allows for the evaluation of the repeatable model bias and variability of the site response models. This incorporates both fixed and random effects to describe the trends in correlated data when grouped by one or more classification factors. In this context, mixed-effect regression accounts for multiple ground motion observations at a single site. Prior work by Bradley (2011) Lin et al. (2011) and Kaklamanos (2013, 2015) used the model defined by Equation 7, for similar studies including site response analyses validation and ground-motion prediction equations.

$$PSA_{res}(T)_{i,j} = a + \eta_{Si} + \epsilon_{i,j} \qquad [7]$$

where *i* refers to a ground motion observation, *j* is a site, *a* is the population mean (fixed-effect), η_{Si} is the inter-site residual (between-site residual), and $\epsilon_{i,j}$ is the intra-site residual (intra-site residual). The three regression parameters used to quantify the uncertainties are the fixed-effect *a,* to represent the model bias, the inter-site standard deviation τ_S, which represents the site-to-site variability and the intra-site standard deviations $\sigma_{0,}$ which accounts for the variability within a single site. These were then combined to compute the total standard deviation ($\sigma_Y = \sqrt{\sigma_0{}^2 + \tau_S{}^2}$) of the site response models.

Finally, the accuracy of the predictions of each modelling approach was quantified using Pearson's correlation coefficient r by comparing the observed and predicted amplification spectra. The methodology employed was based on Thompson et *al*. (2012) and consists in selecting 200 logarithmically spaced frequencies between the first and fourth peak of the site's linear 1D transfer function. In general, r >0.6 is associated with a good correlation between the studied variables. In this study, the coefficients were computed and separated for comparison based on the ratio of peak ground velocity *PGV* over $V_{s\text{-}30}$, which is used as a proxy for the level of shear strain, and the level of pore pressure buildup.

5 RESULTS AND DISCUSSION

5.1 Detailed case study

Ground response analyses were conducted to evaluate and compare the predictions of EQL, NL-TS and NL-ES models for the 1987 Superstition Hills Earthquake (M_w=6.6 & $PGA_{obs\text{-}surf}$=0.19*g*) that triggered liquefaction at the WLA site. A brief description of the studied site was made previously and is available in Section 2. The pore pressure generation model used for this example is the GMP model (M2 - Equation 3), with α =1, v =1 and the relative densities were determined using general correlation relationships based on SPT data.

The results show that effective stress analysis successfully predicts the observed triggering of liquefaction as shown in Figure 1(e). Liquefaction leads to a complete

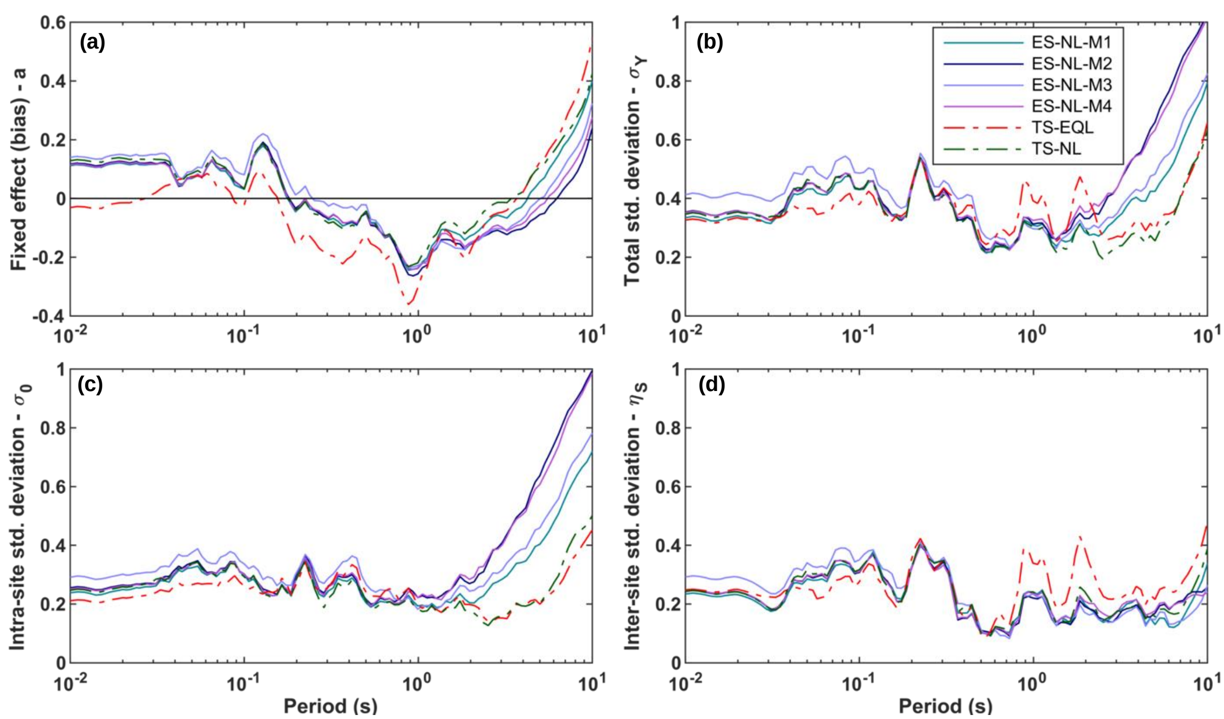

Figure 2. Period dependence of the mixed effect regression analysis across all sites and ground motions. Results from EQL, NL-TS and NL-ES analysis: (a) Model bias or fixed effect *a*, (b) Total standard deviation σ_Y, (c) Intra-site standard deviation σ_0 and (d) Inter-site standard deviation η_S.

loss of the soil's stiffness and strength which is revealed by the presence of peaks of maximum shear strains that reach a maximum of 11% in the liquefiable layer as shown in Figure 1(d). In terms of the response spectra, results in Figure 1(b) indicate that all analyses exhibit a positive bias at short periods and that total stress analyses (EQL & NL-TS) under-predict the motion for periods longer than 0.8s. Although NL-ES analysis captures liquefaction effects from 0.8s to 3s, there is an overprediction of the motion for longer periods. Figure 1(c) shows the acceleration time histories and illustrates how total stress analyses neglect liquefaction effects, while NL-ES simulations are able to capture some of the change in the frequency content of the motion. However, based on these results, NL-ES does not accurately represent the observed behaviour because of an overestimation of soil softening and degradation from the pore pressure generation model.

5.2 Quantification of uncertainty

Residuals are computed for all modelling approaches across all sites and ground motions, and mixed-effect regression analysis are presented in Figure 2 in terms of bias (a) and variability (b-d). Note that the results of different effective stress calibration are grouped by model. For all panels, the results suggest no significant differences between NL-TS and NL-ES models except at periods longer than 1s. When liquefaction occurs, the response of the effective stress model shifts the frequency content toward lower frequencies as noted previously in Section 5.1. The results from Figure 2(a) show that all models except EQL exhibit a positive model bias at periods shorter than 0.2s, as found by previous studies (Kwok et *al*., 2008, Kim and Hashash 2013, Kaklamanos et *al.*, 2015).

Regarding the variability of the residuals, the main finding is that effective stress models significantly increase the intra-site standard deviation at long periods compared with total stress models, which represents the ground-motion variability once all repeatable effects are removed, particularly for the M2 and the M4 models which are both energy-based. Compared with EQL analysis, although nonlinear models have higher intra-site variability for periods shorter than 0.1s, there is a decrease in the inter-site variability at periods higher than 0.6s. In summary, these results do not indicate a clear improvement in the precision of the predictions when using effective stress over total stress models in liquefaction problems and reveal a significant increase in the variability at long periods.

5.3 Accuracy of the predictions

Pearson's correlation coefficients r are computed for each analysis as plotted in Figure 3 and binned in terms of the ratio *of PGV* of the observed downhole motion to $V_{s\text{-}30}$, termed the shear strain index (I_γ) by Idriss (2011), which is representative of the level of nonlinearity encountered in the soil profile for a given motion. Figure 3 demonstrates the benefits of using more advanced nonlinear models as opposed to the common equivalent linear approach. The higher nonlinear r values observed for 7.5e-4 ≤ I_γ ≤ 1e-3 might be associated with the low number of motions contained in the bin. In general, for all values of I_γ, the

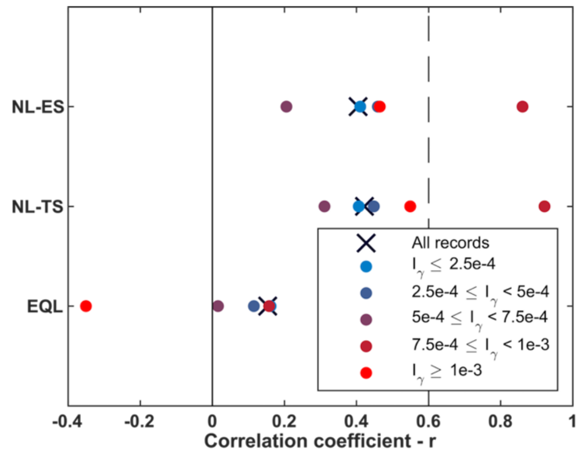

Figure 3. Correlation coefficients between the observed and predicted amplification spectra for EQL, NL-TS and NL-ES analyses binned by the shear strain index (I_γ).

results from TS and ES analysis follow similar tendencies, although, nonlinear effective stress analysis appears to slightly decrease the accuracy of the predictions compared with nonlinear total stress analysis for $I_\gamma \geq$ 2.5e-4. This is likely associated with the overestimation of soil softening, and the tendency of the models to predict liquefaction even when it was not observed.

The coefficients are then computed again for the effective stress analysis and based on the estimated pore pressure ratio r_u as presented in Figure 4.

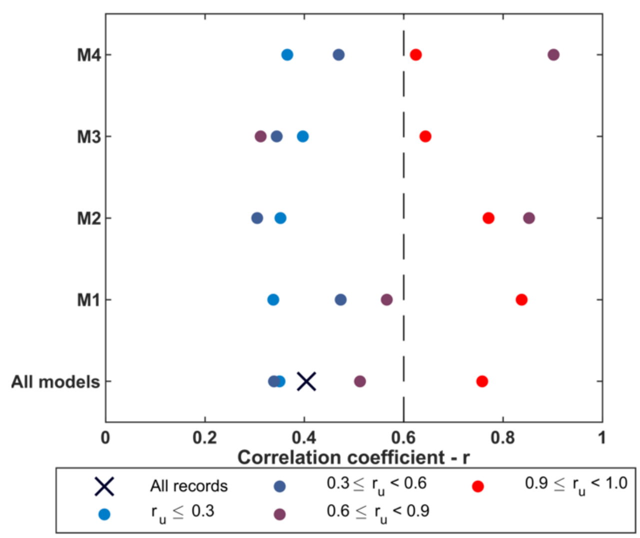

Figure 4. Comparison of correlation coefficients between the observed and predicted spectra for NL-ES analysis (M1, M2, M3, M4) based on the estimated pore pressure ratio r_u.

The results illustrate that the highest r values are obtained for $r_u >$ 0.9 or when triggering of liquefaction is predicted. A significant decrease in the accuracy of the predictions is however observed for all lower levels of pore pressure buildup with r <0.6. This highlights an important bias of the current models, and suggest that they may not be applicable to represent all pore pressure buildup levels since they were mostly calibrated only based on case studies where liquefaction was observed. When comparing the coefficients computed from the different ES models, all the predictions provide similar precision for $r_u < 0.6$, while the computed coefficients for M2 and M4 models reveal a significant improvement for $0.6 < r_u < 0.9$.

6 CONCLUSION

In this study, total stress equivalent linear, nonlinear and effective stress nonlinear 1D ground response analyses were performed and their predictions were compared for 55 ground motion recordings from seven liquefaction case studies. In general, the results indicate that most effective stress models are successful in capturing the triggering of liquefaction when it occurs. However, this study reveals that the models used in effective stress analysis provide less accurate predictions than total stress analysis, increase the variability of the predictions, and tend to predict liquefaction more often than observed. This suggests that current models do not yet represent satisfying tools to use in practice despite the recommendation from the building code. Therefore, this research will serve as the basis for future studies to develop new advanced models capable of capturing pore pressure buildup for a wide range of motion amplitude and soil conditions. From the results of this study, we thus recommend that a rigorous total stress analysis should be prioritized over effective stress analysis given the current state of available constitutive models, in order to avoid inducing additional uncertainty in the predicted ground response, at the expense of the recommendations of the National Building Code of Canada.

Additional analyses not presented herein include the comparisons of predicted and measured, frequency dependent parameters including Arias Intensity, significant durations and predominant spectral or mean period. The pore pressure response of all effective stress constitutive models is also evaluated as a function of time and shear strain and compared with the expected behaviour of liquefiable soils.

7 ACKNOWLEDGMENTS

The authors want to acknowledge the following for providing the strong motion data, site profiles and properties for this study: 1) The National Research Institute for Earth Science and Disaster Prevention (NIED) – KiK-net sites KSRH07 & TCGH16, 2) The Earthquake Engineering Group, Earth Research Institute at University of California, Santa Barbara and United States Geotechnical Survey (USGS) – Wildlife Liquefaction Array, 3) Center for Earthquake Engineering Simulation (CEES), Network for Earthquake Engineering Simulation (NEES) and Professor Scott J. Brandenberg at University of California, Los Angeles – CSP3 centrifuge experiment, 4) Professor Shideh Dashti and Jenny Ramirez at University of Colorado Boulder, Boulder – CFF2 centrifuge experiment, 5) Professor Ahmed-Waeil Elgamal at University of California, San Diego & the Electric Power Research Institute (EPRI) – Lotung Array and 6) Yoshinori Iwasaki – Port Island Array.

8 REFERENCES

Bardet, J. and Kapuskar, M. (1993). Liquefaction sand boils in San Francisco during 1989 Loma Prieta earthquake. *Journal of Geotechnical Engineering*, 119(3): 543–562.

Bennett, M. J., McLaughlin, P. V., Sarmiento, J. S. and Youd, T. L. (1984). Geotechnical investigation of liquefaction sites, Imperial Valley, California. *Open-file Report. 84-252*, U.S. Geological Survey, Washington, D.C.

Berrill, J. and Davis, R. (1985). Energy dissipation and seismic liquefaction of sands: revised model. *Soils and Foundations*, 25(2): 106–118.

Booker, J. R., Rahman, M. S. and Seed, H. B. (1976). GADFLEA: A computer program for the analysis of pore pressure generation and dissipation during cyclic or earthquake loading.

Bradley, B. A. (2011). A framework for validation of seismic response analyses using seismometer array recordings, *Soil Dynamics and Earthquake Eng.*, 31: 512-520.

Brandenberg, S. J., Stewart, J. P. and Afacan, K. (2013). Influence of Liquefaction on Earthquake Ground Motions, *Final Report for USGS Award Number G12AP20098*.

Carlton, B. (2014). An improved description of the seismic response of sites with high plasticity soils, organic clays, and deep soft soil deposits. *PhD Dissertation*. University of California, Berkeley.

Cetin, K. O. and Bilge, H. T. (2012). Cyclic large strain and induced pore pressure models for saturated clean sands. *Journal of Geotechnical and Geoenvironmental. Engineering*, 138(3): 309-323.

Dobry, R., Ladd, R., S., Yokel, F., Y., Chung, R., M. and Powell, D. (1982). Prediction of pore water pressure buildup and liquefaction of sands during earthquakes by the cyclic strain method. *Building science series 138*. Washington, DC: National Bureau of Standards.

Dobry, R. (1985). Liquefaction of soils during earthquakes. Rep. No. CETS-EE-001, National Research Council (NRC), Committee on Earthquake Eng., Washington, DC.

Electrical Power Research Institute, EPRI (1993). “Guidelines for determining design basis ground motions,” *Rpt. No. EPRI TR-102293*, Electrical Power Research Institute, Palo Alto, CA.

Green, R., Mitchell, J. and Polito, C. (2000). An energy-based excess pore pressure generation model for cohesionless soils. *In Proc., John Booker Memorial Symposium*, Sydney, Australia. Balkema Publishers.

Groholski, D. R., Hashash, Y. M., Kim, B., Musgrove, M., Harmon, J. and Stewart, J. P. (2016). Simplified model for small-strain nonlinearity and strength in 1d seismic site response analysis. *Journal of Geotechnical and Geoenvironmental Engineering*, 142(9): 04016042.

Hashash, Y. M. A., Musgrove, M. I., Harmon, J. A., Groholski, D., Phillips, C. A. and Park, D. (2016). DEEPSOIL v6.1. *Technical report*, Urbana, IL.

Idriss, I. M. (2011). Use of Vs30 to represent local site conditions. In *Proceedings of the 4th IASPEI/IAEE international symposium. Effects of source geology on seismic motion,* University of Santa Barbara California, August 23-26th 2011.

Iwasaki, Y. and Tai, M., (1996). Geotechnical aspects of the January 17, 1995 Hyogoken-Nambu Earthquake: Strong motion records at Kobe Port Island, *Soils and Foundations*, Special issue, January: 29-40.

Kaklamanos, J., Bradley, B. A., Thompson, E. M. and Baise, L. G. (2013). Critical parameters affecting bias and variability in site-response analyses using KiK-net downhole array data. *Bulletin of the Seismological Society of America*. 103(3): 1733-1749.

Kaklamanos, J., Baise, L. G., Thompson, E. M. and Dorfmann, L. (2015). Comparison of 1D linear, equivalent-linear and nonlinear site response models at six KiK-net validation sites. *Soil Dynamics and Earthquake Engineering*. 69: 207-219.

Kayen, R., Moss, R. E. S., Thompson, E. M., Seed, R. B., Cetin, K. O., Der Kiureghian, A., Tanaka, Y. and Tokimatsu, K. (2013). Shear-wave velocity-based probabilistic and deterministic assessment of seismic soil liquefaction potential. *Journal of Geotechnical and Geoenvironemental Engineering*, 139(3): 407-419.

Kim, B. and Hashash, Y. M. A. (2013). Site response analysis using downhole array recordings during the March 2011 Tohoku-Oki Earthquake and the effect of long-duration ground motions. *Earthquake Spectra*, 29(1); 37-54.

Kirkwood, P. and Dashti, S. (2018). A centrifuge study of seismic structure-soil-structure interaction on liquefiable ground and implications for design in dense urban areas. *Earthquake Spectra*, 34(3): 1113–1134.

Kramer, S. L., Sideras, S. S., Greenfield, M. W. and Hushmand, B. (2018). Liquefaction, ground motions, and pore pressures at the Wildlife Liquefaction Array in the 1987 Superstition Hills Earthquake. *Geotechnical Earthquake Engineering and Soil Dynamics V*, GEESDV 2018.

Kwok, A. O. L., Stewart, J. P. and Hashash, Y. M. A. (2008). Nonlinear ground-response analysis of Turkey Flat shallow stiff-soil site to strong ground motion. *Bulletin of the Seismological Society of America*; 98(1): 331–343.

Ladd, C. C. (1991). Stability evaluation during staged construction. *Journal of Geotechnical Engineering*, 98: 331-343.

Lee, K. L. and Albaisa, A. (1974). Earthquake induced settlements in saturated sands. *Journal of Geotechnical and Geoenvironmental Engineering*, 100 (Proc Paper 10496).

Lin, P.-S., Chiou, B., Abrahamson, N., Walling, M., Lee, C.-T. and Cheng, C.-T. (2011). Repeatable source, site, and path effects on the ground-motion prediction, *Bulletin of the Seismological Society of America*, 101: 2281-2295.

Matasović, N. (1993). Seismic response of composite horizontally-layered soil deposits. *PhD Dissertation*. University of California, Los Angeles.

Matasović, N. and Vucetic, M. (1995). Generalized cyclic-degradation-pore-pressure generation model for clays. *Journal of Geotechnical Engineering*, 121(1): 33–42.

Mei, X., Olson, S. M. and Hashash, Y. M. (2018). Empirical porewater pressure generation model parameters in 1-d seismic site response analysis. *Soil Dynamics and Earthquake Engineering*, 114: 563–567.

Olarte, J., Paramasivam, B., Dashti, S., Liel, A. and Zannin, J. (2017). Centrifuge modeling of mitigation-soil-foundation-structure interaction on liquefiable ground. *Soil Dynamics and Earthquake Engineering*, 97: 304–323.

Park, T. and Anh, J. (2013). Accumulated stress-based model for prediction of residual pore pressure. In *Proceedings of the 18th International Conference on Soil Mechanics and Geotechnical Engineering*.

Phillips, C. and Hashash, Y. M. A. (2009). Damping formulation for nonlinear 1D site response analyses. *Soil Dynamics and Earthquake Engineering*, 29(7), 1143-1158.

Polito, C. P., Green, R. A. and Lee, J. (2008). Pore pressure generation models for sands and silty soils subjected to cyclic loading. *Journal of Geotechnical and Geoenvironmental Engineering*, 134(10):1490–1500.

Pyke, R., Seed, H. and Chan, C. (1975). Settlement of sands under multidirectional shaking. *Journal of Geotechnical and Geoenvironmental Engineering*, 101(ASCE# 11251 Proceeding).

Seed, H. B., Pyke, R. and Martin, G. R. (1975). Effect of multi-directional shaking on liquefaction of sands. Earthquake Engineering Research Center, *Report No. EERC 75-41*, University of California.

Silver, M. L. and Seed, H. B. (1971). Volume changes in sands during cyclic loading. *Journal of Soil Mechanics and Foundations Div.*, 97(9): 1171-1182.

Stockwell, R. G., Mansinha, L. and Lowe, R. (1996). Localization of the complex spectrum: the S transform. *IEEE transactions on signal processing*, 44(4): 998–1001.

Thompson, E. M., Baise, L. G., Tanaka, Y. and Kayen, R. E. (2012). A taxonomy of site response complexity. *Soil Dynamics and Earthquake Engineering*, 41: 32–43.

Vucetic, M. and Dobry, R. (1986). Pore pressure buildup and liquefaction at level sandy sites during earthquakes. *Research report CE-86-3*. Dept. Civil Eng., Rensselaer Polytechnic Institute, New York.

Wilson, D., Boulanger, R. W. and Kutter, B. L. (2000). Observed seismic lateral resistance of liquefying sand. *Journal of Geotechnical and Geoenvironmental Engineering*, 126(10): 898-906.

Youd, T. L. (1972). Compaction of sands by repeated shear straining. *Journal of Soil Mechanics & Foundation*s Div., 98(7).

Youd, T. L. and Holzer., T. L. (1994). Piezometer Performance at Wildlife Liquefaction Site, California, *Journal of Geotechnical Engineering*, ASCE, 120(6): 975–995.

Youd, T. L., Steidl, J. H. and Nigbor, R. L. (2004). Lessons Learned and the Need for Instrumented Liquefaction Sites, *Soil Dynamics and Earthquake Engineering*, 24 (9-10), 639-646.

Zhang, J., Andrus, R. D. and Juang, C. H. (2005). Normalized shear modulus and material damping ratio relationships. *Journal of Geotechnical and Geoenvironmental Engineering*, 131(4): 453–464.